10-2005

Interaction Of Porphyrins With A Dendrimer Template: Self-aggregation Controlled By Ph

Pavel Kubat

Kamil Lang

Pavel Janda

Pavel Anzenbacher Jr.
Bowling Green State University, pavel@bgsu.edu

Interaction of Porphyrins with a Dendrimer Template: Self-Aggregation Controlled by pH

Pavel Kubát,[†] Kamil Lang,[‡] Pavel Janda,[†] and Pavel Anzenbacher, Jr.*,[§]

J. Heyrovský Institute of Physical Chemistry, Academy of Sciences of the Czech Republic, Dolejškova 3, 182 23 Prague 8, Czech Republic, Institute of Inorganic Chemistry, Academy of Sciences of the Czech Republic, 250 68, Řež, Czech Republic, and Department of Chemistry and Center for Photochemical Sciences, Bowling Green State University, Bowling Green, Ohio 43403

Received April 25, 2005. In Final Form: July 28, 2005

The interaction between self-aggregated porphyrins such as 5,10,15,20-tetrakis(4-sulfonatophenyl)-porphyrin (**TPPS**) and 5,10,15,20-tetrakis(4-phosphonatophenyl)porphyrin (**TPPP**), and a generation 5 (**G5**) PAMAM dendrimer template is governed by minute differences of porphyrin acido-basic properties. While at neutral pH both monomeric **TPPS** and **TPPP** form complexes with **G5**, decreasing pH did not lead to porphyrin ring protonation ($pK_a \approx 5$) but rather to the preferential formation of H-aggregates (probably H-dimers), most likely due to protonation of the **G5**. Upon further acidification of the solution, this face-to-face orientation of the porphyrin units is being converted to edge-to-edge aligned J-aggregates with a tightly defined structure. This process starts by protonation of the porphyrin ring at pH below 2.3 and 2.8 for **TPPS** and **TPPP**, respectively. The AFM imaging of porphyrin/**G5** nanostructures obtained at pH 0.7 shows the formation of long nanorods of **TPPS** with partially aggregated **G5** and small aggregates of **TPPP** connected to individual **G5** molecules.

Introduction

Various porphyrin derivatives have attracted considerable interest over the past decades due to their interesting structural, optical, and electrical properties, and applications ranging from medicine to materials chemistry.[1] Porphyrins are widely studied in optical applications involving photodynamic therapy (PDT) of tumors[2] and light energy harvesting in artificial photosynthetic processes,[3] as well as for their ability to function as sensors,[4] molecular sieves,[5] catalysts,[6] and biomineralization templates.[7] The well-developed synthetic chemistry in the porphyrin field has rendered the compounds synthetically adaptable to complex supramolecular assemblies.[8] Owing both to their planarity and high polarizability, porphyrins often show a strong tendency to self-aggregate and to form highly complex nanostructures.[9−11]

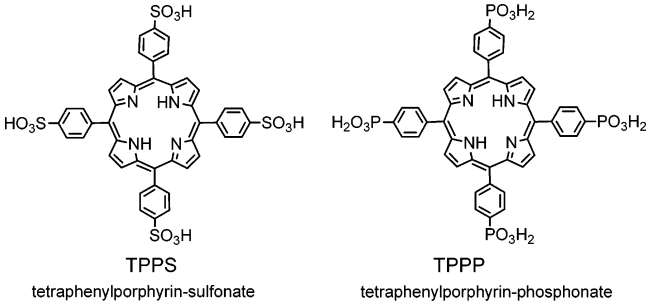

Poly(amidoamine) (PAMAM) dendrimers and their derivatives may be used as carrier systems for drug delivery.[12] Their size and structure can be controlled by synthetic means and they can easily be processed and made biocompatible and biodegradable.[13] In addition,

* To whom correspondence should be addressed. Tel: (419) 372-2080. Fax: (419) 372-9809. E-mail: pavel@bgnet.bgsu.edu.

† J. Heyrovsk'y Institute of Physical Chemistry.

‡ Institute of Inorganic Chemistry.

§ Bowling Green State University.

(1) Kadish, K.; Smith, K. M.; Guillard, R. *The Porphyrin Handbook*; Academic Press: New York, 1999.

(2) Patrice T. *Photodynamic Therapy*; Royal Society of Chemistry: London, 2004.

(3) (a) Wasielewski, M. R. *Chem. Rev.* **1992**, *92*, 435−461. (b) Abdelrazzaq, F. B.; Kwong, R. C.; Thompson, M. E. *J. Am. Chem. Soc.* **2002**, *124*, 4796−4803. (c) Yamada, H.; Imahori, H.; Nishimura, Y.; Yamazaki, I.; Ahn, T. K.; Kim, S. K.; Kim, D.; Fukuzumi, S. *J. Am. Chem. Soc.* **2003**, *125*, 9129−9139.

(4) (a) Lee, W. W.; Wong, K.; Li, X.; Leung, Y.; Chan, C.; Chan, K. S. *J. Mater. Chem.* **1993**, *3*, 1031−1035. (b) Rakow, N. A.; Suslick, K. S. *Nature* **2000**, *406*, 710−713. (c) Smith, V. C.; Batty, S. V.; Richardson, T.; Foster, K. A.; Johnstone, R. A. W.; Sobral, A. J. F. N.; Gonsalves, A. M. d. A. R. *Thin Solid Films* **1996**, *284−285*, 911−914.

(5) (a) Belanger, S.; Hupp, J. T. *Angew. Chem., Int. Ed. Engl.* **1999**, *38*, 2222−2224. (b) Keefe, M. H.; O'Donnell, J. L.; Bailey, R. C.; Nguyen, S. T.; Hupp, J. T. *Adv. Mater.* **2003**, *15*, 1936−1939.

(6) (a) Gonsalves, A. M. D. R.; Pereira, M. M. *J. Mol. Catal. A* **1996**, *113*, 209−221 and references therein. (b) Merlau, M. L.; Mejia, M. P.; Nguyen, S. T.; Hupp, J. T. *Angew. Chem., Int. Ed.* **2001**, *40*, 4239−4242.

(7) Xu, G.; Yao, N.; Aksay, I. A.; Groves, J. T. *J. Am. Chem. Soc.* **1998**, *120*, 11977−11985.

(8) Steed, J. W.; Atwood, J. L. *Supramolecular Chemistry*, Wiley: Chichester UK, 2000.

(9) (a) Rotomskis, R.; Augulis, R.; Snitka, V.; Valiokas, R.; Liedberg, B. *J. Phys. Chem. B* **2004**, 2833−2838. (b) Schwab, A. D.; Smith, D. E.; Rich, C. S.; Young, E. R.; Smith, W. F.; de Paula, J. C. *J. Phys. Chem. B* **2003**, *107*, 11339−11345. (c) Crusats, J.; Claret, J.; Diez-Perez, I.; El-Hachemi, Z.; Garcia-Ortega, H.; Rubires, R.; Sagues, F.; Ribo, J. M. *Chem. Commun*. **2003**, 1588−1589. (d) Chen, X.; Drain, Ch. M. In *Encyclopedia of Nanoscience and Nanotechnology;* Nalwa, H. S., Eds.; American Scientific Publishers: Stevenson Ranch, CA, 2004; Vol.9, p 593. (e) Ogawa, K.; Kobuke, Y. In*. Encyclopedia of Nanoscience and Nanotechnology*; Nalwa, H. S., Eds.; American Scientific Publishers: Stevenson Ranch, CA, 2004; Vol.9, p 561.

(10) (a) Kubát, P.; Lang, K.; Anzenbacher, P., Jr. *J. Phys. Chem. B* **2002**, *106,* 6784−6792. (b) Kubát, P.; Lang, K.; Procházková, K.; Anzenbacher, P., Jr. *Langmuir* **2003**, *19*, 422−428.

(11) (a) Micali, N.; Mallamace, F.; Romeo, A.; Purrello, R.; Scolaro, L. M. *J. Phys. Chem B* **2000**, *104*, 5897−5904. (b) Kano, K.; Fukuda, K.; Wakami, H.; Nishiyabu, R.; Pasternack, R. F. *J. Am. Chem. Soc.* **2000**, *122*, 7494−7502.

(12) (a) Haag, R. *Angew. Chem., Int. Ed*. **2003**, *43*, 278−282. (b) Duncan, R. *Polym. Mater. Sci. Eng*. **2001**, *84*, 214. (c) Esfand, R.; Tomalia, D. A. *Drug Disc. Today* **2001**, *6*, 427−436.

(13) Luo, D.; Haverstick, K.; Belcheva, N.; Han, E.; Saltzman, W. M. *Macromolecules* **2002**, *35*, 3456−3462.

10.1021/la051106g CCC: $30.25
Published on Web 09/13/2005

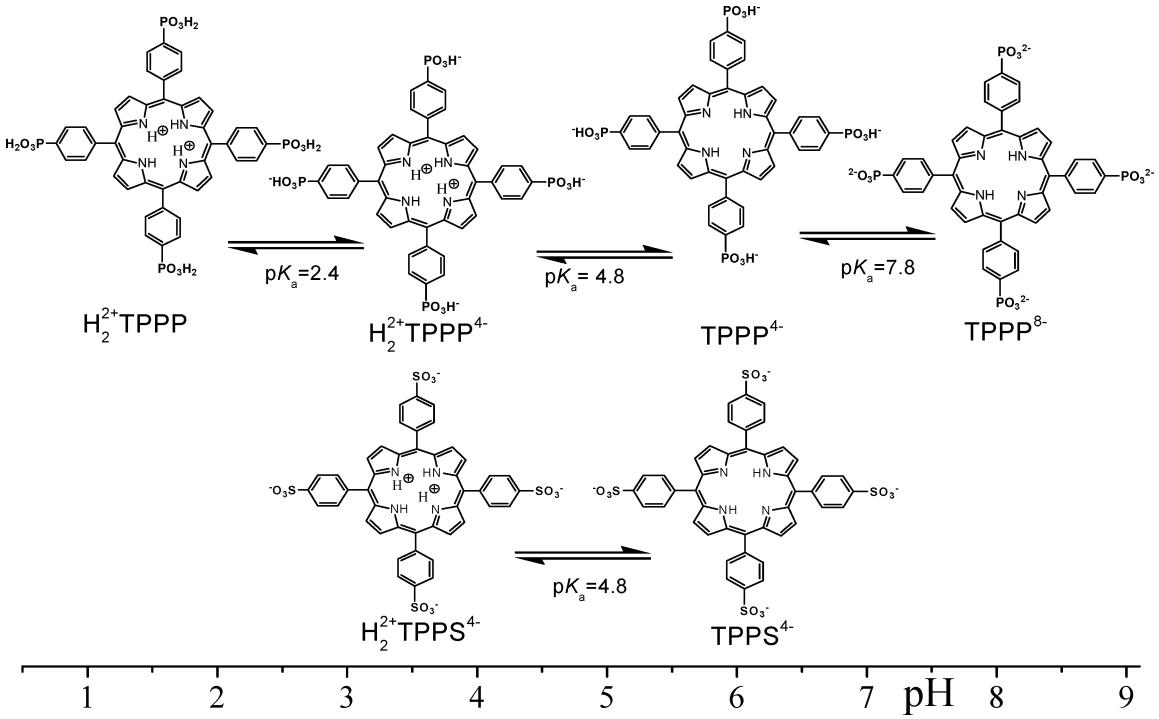

Figure 1. Acido-basic properties of free porphyrins **TPPS** and **TPPP**.

while they can be used to encapsulate individual small drug molecules in the manner of polymer micelles, they can also serve as reservoirs for drug molecules that can be attached or embedded within their structure using covalent bonds or perhaps even noncovalent interactions. A practical result of such ability would be that a single dendrimer may potentially be used to transport a large number of drug molecules. The transport of porphyrin derivatives is one of the necessary conditions for successful porphyrins-mediated PDT.[2,14] The potential application of dendrimers as porphyrin carriers is predicated upon detailed understanding of the porphyrin-dendrimer association, which is the subject-matter of this study.

Porphyrin aggregates can be classified according to the orientation of the induced transition dipole of the constituent monomers and the corresponding position of the Soret band in the UV−vis spectrum.[15,16] The Soret band position for cofacial aggregates (H-aggregates) is blue-shifted, whereas for the edge-to-edge aggregates (J-aggregates) it is red-shifted with respect to the absorption of the monomer. The origin of these features is explained by the formation of an excitonic state through the electronic coupling of tightly packed porphyrin units.[17,18] The formation of porphyrin aggregates in aqueous solutions is affected by the structure and substitution of the respective porphyrin, ionic strength, temperature, pH, and the presence of molecular templates. We decided to investigate the role of PAMAM dendrimers, highly branched, amine-terminated, spherical macromolecules, characterized by narrow size distribution and a high degree of molecular uniformity.[19,20] The properties of PAMAM dendrimers in an aqueous solution are significantly influenced by pH.[21,22] At neutral pH, when all the primary amines are protonated (pK_a = 9.0−10.7), the radius of gyration for generation 5 (**G5**) PAMAM is 5.4 nm. At pH below 3, tertiary amines are also largely protonated, which results in 30−40% increase in the radius of gyration due to the repulsive Coulombic forces.

In this paper, we describe interesting pH-dependent aggregation of porphyrins in the presence of **G5**. We selected two porphyrins with different acido-basic behavior and also by the self-aggregation mechanism in an aqueous solution.[23,24]

In acidic solutions, 5,10,15,20-tetrakis(4-sulfonatophenyl)porphyrin, **TPPS** (Figure 1), forms J-aggregates after protonation of the porphyrin ring from H_2^{2+}TPPS^{4-}, while 5,10,15,20-tetrakis(4-phosphonatophenyl)porphyrin, **TPPP** (Figure 1), can form self-aggregates originating from two different forms, H_2^{2+}TPPP^{4-} and H_2^{2+}TPPP. Previous literature data for interaction of TPPS^{4-} with **G2** and **G4** show its tendency to form H-aggregates at pH 7 at high porphyrin loading as well as the formation of H_2^{2+}TPPS^{4-} J-aggregates at pH 2.[25,26] The decrease of pH result in protonation of both the dendrimer surface and to some extent also the interior, PAMAM dendrimer is capable of acting as a template for porphyrin aggregation even at porphyrin concentrations under which both **TPPS** and **TPPP** do not form aggregates at pH 7. Thus,

(14) (a) Vicente, M. G. H. *Curr. Med. Chem.: Anti-Cancer Agents* **2001**, *1*, 175−194. (b) Rousset, N.; Bourre, L.; Thibaud, S. *Comprehensive Series in Photochemistry & Photobiology* **2003**, Vol. 2 (Photodynamic Therapy), 59−80.
(15) Kasha, M. *Radiat. Res.* **1963**, *20*, 55−70.
(16) Ribó, J. M.; Bofill, J. M.; Crusats, J.; Rubires, R. *Chem. Eur. J.* **2001**, *7*, 2733−2737.
(17) Frank, J.; Teller, E. *J. Chem. Phys.* **1938**, *6*, 861−872.
(18) Ohno, O.; Kaizu, Y.; Kobayashi, H. *J. Chem. Phys*. **1993**, *99*, 4128−4139.
(19) Tomalia, D. A.; Baker, H.; Dewald, J. R.; Hall, M.; Kallos, G.; Martin, S.; Roeck, J.; Ryder, J.; Smith, P. *Macromolecules* **1986**, *19*, 2466−2468.
(20) Bosman, A. W.; Janssen, H. M.; Meijer, E. W. *Chem. Rev.* **1999**, *99*, 1665−1688.
(21) Maiti, P. K.; Çagin, T.; Lin, S.; Goddard, W A., III. *Macromolecules* **2005**, *38*, 979−991.
(22) Diallo, M. S.; Christie, S.; Swaminathan, P.; Balogh, L.; Shi, X.; Um, W.; Papelis, Ch.; Goddard, W., III; Johnson, J. H., Jr. *Langmuir* **2004**, *20*, 2640−2451.
(23) De Napoli, M.; Nardis, S.; Paolesse, R.; Vicente, M. G. H.; Lauceri, R.; Purrello, R. *J. Am. Chem. Soc*. **2004**, *126*, 5934−5935.
(24) Kubát, P.; Lang, K.; Anzenbacher, P., Jr. *Biophys. Biochem. Acta* **2004**, *1670*, 40−48.
(25) Paulo, P. M. R.; Costa, S. M. B. *Photochem. Photobiol. Sci*. **2003**, *2*, 597−604.
(26) Paulo, P. M. R.; Gronheid, R.; DeSchryver, F. C.; Costa, S. M. B. *Macromolecules* **2003**, *36*, 9135−9144.

indirectly, pH may be used to control the structure of the porphyrin self-aggregates.

Experimental Section

5,10,15,20-tetrakis(4-sulfonatophenyl)porphyrin tetrasodium salt (**TPPS**) and generations 5 (**G5**) and 0 **(G0)** of PAMAM (all Aldrich) in a methanol solution were used as purchased. The synthesis of 5,10,15,20-tetrakis(4-phosphonatophenyl)porphyrin (**TPPP**) has been described in our previous paper.[24] The apparent binding constants K_b for porphyrin−**G0** complexes were calculated using the Benesi−Hildebrant plots constructed from the absorbance changes at the Soret maximum assuming a 1:1 stoichiometry and using the concentration of **G0** significantly larger than that of a porphyrin.[27]

UV−vis absorption spectra were recorded using a Perkin-Elmer Lambda 19 spectrophotometer, and steady-state fluorescence emission spectra using a Perkin-Elmer LS 50B luminescence spectrophotometer. Resonance light-scattering experiments (RLS) were performed using simultaneous scans of the excitation and emission monochromators in the range of 300−600 nm. A Lambda Physik FL 3002 dye laser (λ_{exc} = 414−440 nm, pulse length 28 ns, output 0.1−5 mJ/pulse) was used to generate the triplet states. Transient spectra were recorded using a laser kinetic spectrometer (Applied Photophysics, UK). Time profiles of the triplet state decay were recorded at 450 and 500 nm using a 250 W Xe lamp equipped with a pulse unit, and a R928 photomultiplier (Hamamatsu). The samples were saturated by air or by oxygen and, where appropriate, oxygen was removed from the solution via argon purging.

The porphyrin/**G5** nanostructures were imaged using a tapping mode AFM (Nanoscope IIIa, Veeco, USA). The nanostructures were prepared by casting a droplet (20−50 μL) of a porphyrin solution onto the basal plane of a highly ordered graphite (HOPG grade SPI-2, SPI, USA) substrate. The droplet was removed after 10 s. The sample was then dried in ambient air.

Results and Discussion

Binding of TPPS and TPPP at pH 7.0. At pH 7.0, the **TPPS** and **TPPP** UV−vis spectra show the characteristic features of a porphyrin free base. The absorption spectra are composed of the Soret band at 413 for **TPPS** and 414 nm for **TPPP**, and four Q-bands around 516, 553, 580, and 633 nm. The effects of interaction between the title porphyrins and **G5** strongly depend on the porphyrin/**G5** molar ratio. This is reflected by the UV−vis and fluorescence spectra. At a molar excess of **G5**, both **TPPS** and **TPPP** show a red shift of the Soret band to 420 nm (Q-bands at 518, 553, 590, and 646 nm) and 422 nm (Q-bands at 519, 555, 591, and 646 nm), respectively, indicating the binding of the porphyrin monomeric units at positively charged amine termini of **G5** (Figure 2b,d). This observation is supported by corresponding shifts in fluorescence spectra observed for both Q-bands from 644 and 705 nm to 651 and 716 nm for **TPPS**, and from 645 and 705 nm to 654 and 718 nm for **TPPP**, respectively. The results of UV−vis and fluorescence spectroscopy measurements are similar to those described for **TPPS** with **G4** in PBS buffer at pH 7.[25,26]

Transient triplet−triplet spectra of **TPPS** and **TPPP** show typical broad absorption maxima at 450 nm not affected by the binding processes (Figure 3c). In air-saturated solutions, the triplet states of the bound monomer are quenched by oxygen monoexponentially with the lifetime of 12.0 ± 0.2 μs (Figure 3b). The triplet state lifetimes are ca. 7 times longer than the ones observed for free porphyrin molecules (1.7 ± 0.1 μs, Figure 3a). The increase in the triplet lifetime after the binding to a large molecule is attributed to a combination of several factors including the confinement of the excited molecule within

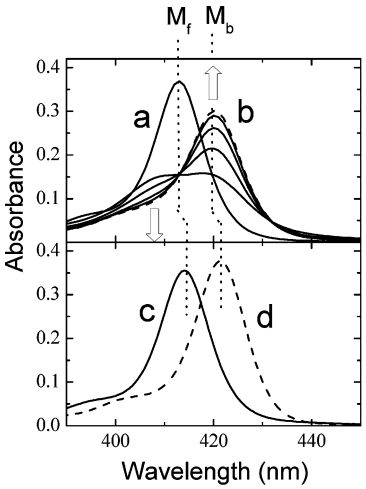

Figure 2. Effect of **G5** on the Soret band of **TPPS** and **TPPP** (1.1 μM solution in 20 mM phosphate buffer, pH 7.0): (a) free **TPPS**, (b) **TPPS** in the presence of 0.3, 1.6, 3.2, 4.8, 8.5 (dashed line) μM **G5**, (c) free **TPPP**, and (d) **TPPP** in the presence of 9.2 μM **G5** (dashed line). The arrows show changes induced by increasing concentration of **G5**. M_b designates the monomer bound to **G5**; M_f represents a free porphyrin monomer in the solution.

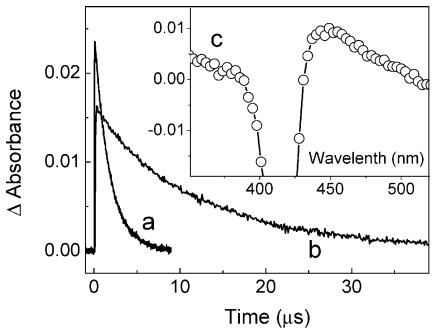

Figure 3. Formation of the triplet states after excitation by a 420 nm pulse recorded at 450 nm in 20 mM phosphate buffer, pH 7.0: (a) for **TPPS**, (b) **TPPS** bound to **G5**. The corresponding difference absorption spectrum at 1 μs is shown in the inset.

the solvent shell and changes in the solvent−solute interactions due to reduced exposure of the excited molecules to solvent molecules.[28]

To obtain quantitative insight into the forces driving the association between **TPPS** or **TPPP** and dendrimer amine groups, a simple model comprising four terminal amine groups (**G0**) was investigated. At pH 7.0 all terminal amino-groups are protonated. During titration of porphyrins by **G0** a red shift of the Soret bands indicating the formation of the bound porphyrin monomer was observed, vide supra. The appearance of a clear isosbestic point typical for the presence of two porphyrin forms in a solution, a free porphyrin and a porphyrin bound to **G0**, was also observed. The **G0**-porphyrin binding constants (K_b) calculated from these titration experiments were (3.4 ± 0.4) × 10^3 M^{-1} for **TPPS** and (4.0 ± 0.6) × 10^3 M^{-1} for **TPPP**, respectively.

At high molar porphyrin/**G5** ratios (>1) the Soret band is split and then hypsochromically shifted to 410 nm, indication that the positively charged **G5** exterior imposes structural packing (or monomer compaction/aggregation) of **TPPS** and **TPPP** (Figure 2a,b). The described spectral changes are typical for the face-to-face arrangement of

(27) Connors, K. A. *Binding Constants, The Measurement of Molecular Complex Stability*; John Wiley & Sons: New York, 1987; pp. 141−187.

(28) Lang, K.; Mosinger, J.; Wagnerová, D. M. *Coord. Chem. Rev.* **2004**, *248*, 321−350.

the porphyrin units in H-type aggregates.[15,16] The formation of porphyrin aggregates on the surface of the **G5** template is controlled by electrostatic and hydrophobic interactions. The probability, p_i, of finding i porphyrin molecules in a single **G5** is described by the Poisson statistics, $p_i = r^i e^{-r}/i!$, where r is the average number of porphyrin molecules per dendrimer. For the equimolar porphyrin/**G5** ratio ($r = 1.0$) the probabilities that a single **G5** contains one, two, three, four, and more than four porphyrin molecules are 0.368, 0.184, 0.061, 0.015, and less than 0.007, respectively. This suggests that the aggregate structures are most probably H-dimers rather than H-oligomers. This conclusion is also supported both by the appearance of an isobestic point during titration of porphyrins by **G5** (Figure 2a,b), which is typical for the equilibrium of only two light-absorbing components (one is a bound monomer), as well as the RLS measurements. The latter technique allows identification of extended aggregated species even at low concentrations as the amount of scattered light is directly proportional to the volume of particles and monomeric molecules and small oligomers show no enhanced scattering.[29] As expected, no RLS signals were observed confirming that the observed aggregates are too small in size to scatter light. This is in agreement with previous observations describing H-type **TPPS** dimers on the surface of **G2** and **G4** dendrimers.[25,26]

The described spectral changes of **TPPS** are accompanied by a shift of the fluorescence emission band from 651 and 716 nm to 664 and 721 nm indicating that the dimeric structure is fluorescent (**TPPP** behaves similarly). Such behavior was observed for H-type dimers in the **TPPS/G4** system at neutral pH,[25,26] aggregated **TPPS** in micelles,[30] or cyanine dyes aggregating on polyelectrolytes,[31] and may be attributed to a deviation from the strict parallel arrangement of transition dipole moments of the porphyrin units.

pH-Driven Formation of H-Aggregates on PAMAM Dendrimer Template. At neutral pH, PAMAM dendrimer-templated H-aggregation can be achieved by increasing the porphyrin/PAMAM dendrimer ratio.[25,26] In this paper, we describe that H-aggregates are formed as a result of pH modulation and how this parameter affects the mode and stoichiometry of the aggregation. We demonstrate how this parameter may be continually changed thus allowing us to control and program the alignment of the porphyrin units. The pH-driven H-aggregation on the **G5** template is evidenced by changes in the UV−vis (Figure 4) and fluorescence spectra. The experiments start in a nonbuffered solution at neutral pH where porphyrin monomers are bound to PAMAM. Although pK_a of the porphyrin pyrrole nitrogens is close to 5 (Figure 1), no protonation of **TPPS** and **TPPP** in the presence of **G5** was observed at pH above 2.3 for **TPPS**, and above 2.8 for **TPPP**, respectively. Instead of potential protonation, at pH 4.0−2.3 for **TPPS** and 4.0−2.8 for **TPPP**, the spectral features show the same behavior described above for a molar excess of porphyrin over PAMAM: a hypsochromically shifted band to 410 nm with an isosbestic point, a shift of the fluorescence emission, and no RLS signals. The same spectroscopic behavior is observed after addition of **G5** into a solution of diprotonated porphyrins (e.g., $H_2^{2+}TPPS^{4-}$, Figure 1) at pH

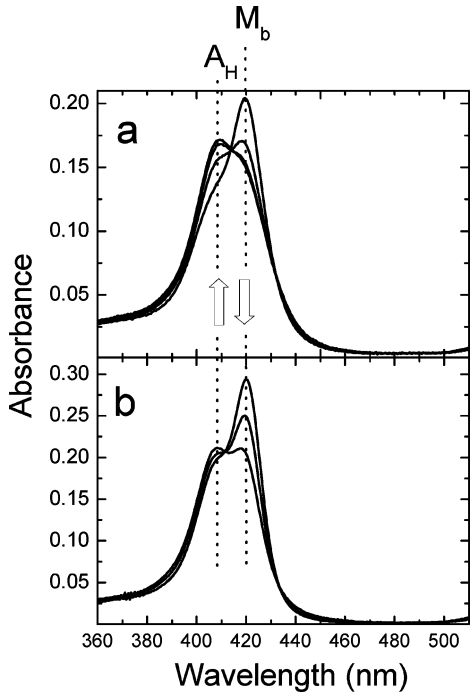

Figure 4. Titration of porphyrins (nonbuffered solution in the presence of 1.8 μM **G5**) by HCl: (a) 1.8 μM **TPPS**, pH 3.3−2.3; (b) 2.2 μM **TPPP**, pH 3.2−2.8. Arrows show changes induced by decreasing pH; M_b designates a monomer bound to **G5** and A_H H-aggregate (dimer).

values higher than 2.3 for **TPPS** and 2.8 for **TPPP** where porphyrin deprotonation upon binding to PAMAM is observed. Also, in comparison to the triplet quantum yields recorded for the monomer, the magnitude of the triplet state formation was found to be significantly lower upon PAMAM addition. This observation supports the notion of aggregation and/or binding, particularly when one considers that the triplet state lifetimes of 12 ± 2 μs in an air-saturated solution (see above) generally do not depend either on pH or the porphyrin peripheral substituents. These results are a strong indication of a decrease in the contribution of the porphyrin monomer M_b bound to **G5** and point to the preferred formation of H-dimers A_H (Figure 4a,b). The data also show that the formation of a dimeric structure at low pH is kinetically controlled, as it depends on the incubation time, rate of the pH change, and intensity of mixing.

At low pH (pH $\approx$ 3) the tertiary nitrogen atoms of PAMAM are mostly protonated (pK_a is between 6.3 and 7.2) and repulsion forces between individual chains create cavities[21,32] suitable for accommodation of negatively charged porphyrins. The association of π-conjugated porphyrin rings is a result of delicate equilibria stemming from the combination of attractive $\sigma-\pi$ and repulsive $\pi-\pi$ interactions.[33] It is, therefore, logical that the porphyrin assemblies (and/or aggregates) can be stabilized by Coulombic interaction between the negatively charged porphyrin periphery and protonated **G5** nitrogen atoms as depicted in Figure 5a. The significance of Coulombic forces for the formation of dimers is demonstrated by the fact that at pH where both **TPPS** and **TPPP** are generally protonated, the protonation does not occur but the H-dimers are stabilized. The extent of H-aggregation also increases with an increasing porphyrin/PAMAM molar

(29) (a) Pasternack, R. F.; Collings, P. J. *Science* **1995**, *369*, 935−939. (b) dePaula, C. C.; Robblee, J. H.; Pasternack, R. F. *Biophys. J.* **1995**, *68*, 335−341.

(30) Maiti, N. C.; Mazumdar, S.; Periasamy, N. *J. Phys. Chem. B* **1998**, *102*, 1528−1538.

(31) Peyratout, C.; Daehne, L. *Phys. Chem. Chem. Phys.* **2002**, *4*, 3032−3039.

(32) Chen, W.; Tomalia, D. A.; Thomas, J. L. *Macromolecules* **2000**, *33*, 9169−9172.

(33) Hunter, C. A.; Sanders, J. K. M. *J. Am. Chem. Soc.* **1990**, *112*, 5525−5534.

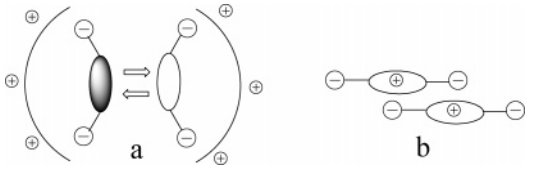

Figure 5. Schematic representation of a possible arrangement of two porphyrin units of the H-dimer inside the **G5** cavity stabilized (a) by electrostatic and hydrophobic forces, and (b) a J-structure stabilized by electrostatic forces.

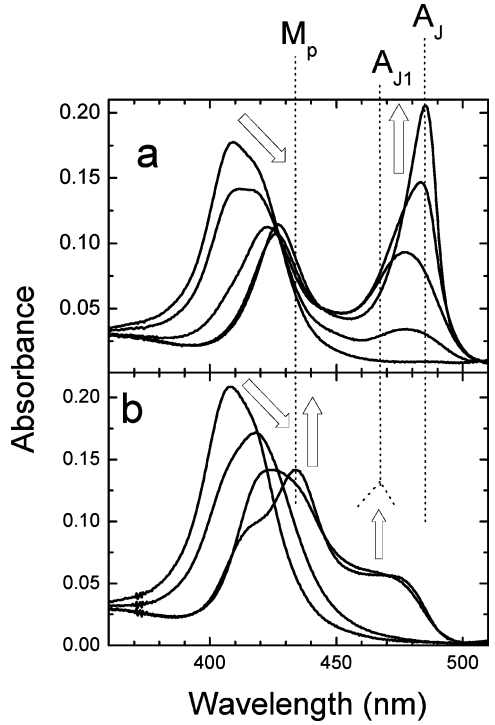

Figure 6. Titration of porphyrins by HCl in the presence of 1.8 μM **G5**: (a) 1.8 μM **TPPS**, pH 2.2−0.9; (b) 2.2 μM **TPPP**, pH 2.5−1.0. Arrows show changes induced by decreasing pH, M_p designates the protonated form of a monomer, A_J and A_{J1} correspond to the J-aggregates.

ratio. This process was also observed at high porphyrin/PAMAM dendrimer ratios even at pH 7.0.[25,26] Under such conditions, however, the tertial amine nitrogens are only partially protonated while fully protonated are only the terminal amine nitrogens.

pH-Driven Formation of J-Aggregates. Further decrease of pH below 2.3 leads to additional spectral changes. The Soret band of **TPPS** originally centered at 410 nm is transformed into new bands at 420, 476, and 691 nm (Figure 6a). Higher porphyrin/**G5** molar concentration ratios, lower pH, or aging of a solution results in further gradual shifting of the absorption peaks to 424, 488, and 701 nm. These spectral features are attributed to a tighter molecular packing of a diprotonated porphyrin ($H_2^{2+}TPPS^{4-}$, Figure 1) leading to a linear assembly formed on the basis of the electrostatic interaction model depicted in Figure 5b.[16,34−36] Since $H_2^{2+}TPPS^{4-}$ is a zwittterionic molecule, the positively charged center of one $H_2^{2+}TPPS^{4-}$ molecule can attract the negatively charged peripheral sulfonated groups of the adjacent molecules. Also, the electrostatic repulsion of the anionic groups is partly shielded by the excess of free cations (high ionic strength)[16,34−36] or by a positively charged matrix.[25,30,37,38]

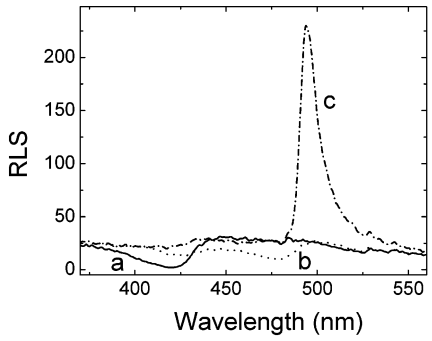

Figure 7. Resonance light-scattering spectra of **TPPS** bound to **G5**: (a) 2.7 μM **TPPS**, 1.4 μM **G5** at pH 7.6; (b) 2.5 μM **TPPS**, 1.3 μM **G5** at pH 1.5; (c) 3.8 μM **TPPS**, 1.3 μM **G5** at pH 1.5.

The appearance of J-aggregates is accompanied by the presence of a protonated TPPS monomer as documented by fluorescence emission bands at 670 nm. Also, the fluorescence excitation spectra recorded at emission of 670 nm reveal the absorption band of $H_2^{2+}TPPS^{4-}$ at 434 nm. The protonation of TPPS occurs at pH below 2.3 and results in the ejection of the $H_2^{2+}TPPS^{4-}$ from the dendrimer cavities due to repulsive Coulombic forces between the positive porphyrin ring and protonated **G5** nitrogen atoms. This ejection is responsible for the conversion of the face-to-face aggregate geometry to J-aggregates (Figure 5b). The dominant presence of J-aggregates is also confirmed by characteristic fluorescence emission at 715 nm. It is interesting to note that the initial broad absorption band at 476 nm develops into narrow exciton absorption centered at 488 nm. Such shifts can be interpreted as a conversion of a solution phase J-aggregate into more organized aggregate particles as a lower number of protonated monomeric species experience perturbation imposed by the porphyrin-dendrimer interaction. Increasing exciton coupling among the porphyrin molecules is also confirmed by the band narrowing, which indicates compaction of a larger number of the monomeric units in the J-aggregates. The latter observation is supported by results of the RLS experiments shown in Figure 7. In the RLS spectra, the bound monomer produces only a minimum at 420 nm (Figure 7a) and the preformed J-aggregate displays a minimum at a 479 nm (Figure 7b) due to self-absorption. The PAMAM dendrimer-induced formation of a compact J-aggregate is then confirmed by a sharp light-scattering signal obtained at 493−494 nm (Figure 7c) and simultaneous narrowing of the Soret band of J-aggregates and shifting its maximum above 484 nm. The intensity of this signal and the rate of its formation depend on several factors including the molar ratio TPPS/**G5**, aging of the mixture, and even the order of the component mixing. The average aggregation number of such J-aggregates is in the range of 10^5−10^6.[39]

Similarly to **TPPS**, the decrease of pH results in the ejection of the **TPPP** H-dimer from the PAMAM assembly; however, broad absorption features in the range of 450−500 nm are generated (Figure 6b) rather than a sharp exciton band as in the case of **TPPS**. This difference

(34) Akins, D. L.; Zhu, H. R.; Guo, C. *J. Phys. Chem.* **1996**, *100*, 5420−5425.

(35) Akins, D. L.; Özcelik, S.; Zhu, H. R.; Guo, C. *J. Phys. Chem.* **1996**, *100*, 14390−14396.

(36) Chen, D. M.; He, T.; Cong, D. F.; Zhang, Y. H.; Liu, F. C. *J. Phys. Chem. A* **2001**, *105*, 3981−3988.

(37) Xu, W.; Guo, H.; Akins, D. L. *J. Phys. Chem. B* **2001**, *105*, 1543−1546.

(38) Jiang, S.; Liu, M. *J. Phys. Chem. B* **2004**, *108*, 2880−2884.

(39) Collings, P. J.; Gibbs, E. J.; Starr, T. E.; Vafek, O.; Yee, C.; Pomerance, L. A.; Pasternack, R. F. *J. Phys. Chem. B* **1999**, *103*, 8474−8481.

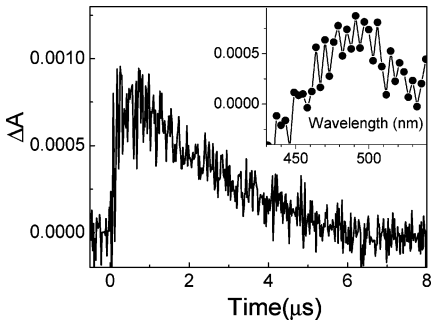

Figure 8. Changes in the absorbance at 500 nm after excitation by a 434 nm pulse due to formation of the triplet states of H_2^{2+}TPPP. The lifetime is 3.2 ± 0.4 μs. Inset: Transient absorption spectrum of H_2^{2+}TPPP recorded 1 μs after excitation. 4.1 μM **TPPP**, 3.2 μM **G5**, pH 1.1.

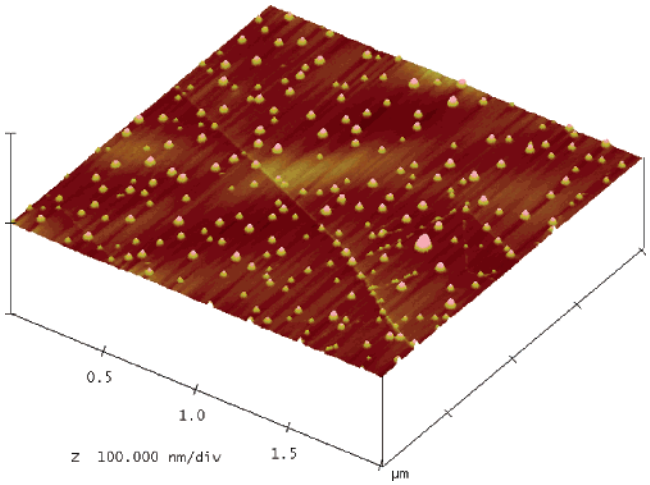

Figure 9. PAMAM dendrimer **G5** deposited by drop casting of its aqueous solution (3.5 μM, pH 0.7) on HOPG basal plane, imaged by AFM tapping mode.

originates in the specific acido-basic equilibria of **TPPP** (Figure 1).[23,24] While the zwitterionic nature of the H_2^{2+}TPPS^{4-} monomer is responsible for Coulombic stabilization of the J-aggregate, since the peripheral phosphate groups in **TPPP** are uncharged (pK_a = 2.4), such a stabilizing factor is not observed in protonated **TPPP**. The resulting broad spectral features together with no RLS signals indicate that the formed J-aggregates are randomly oriented and too small to scatter light. In addition to the red-shifted band of J-aggregates, the newly appeared band at 434 nm is attributed to the free protonated porphyrin monomer H_2^{2+}TPPP (Figure 1). Its concentration is much higher than that of the H_2^{2+}TPPS^{4-} monomer, since H_2^{2+}TPPP is less consumed in J-aggregates. The presence of H_2^{2+}TPPP is further confirmed by the characteristic fluorescence emission band at 675 nm as well as by transient spectroscopy. The kinetic traces of H_2^{2+}TPPP triplet states (Figure 8) were used to construct a transient spectrum with a typical absorption band near 500 nm (Figure 8, inset).[24,40]

Solid-State Studies of Porphyrin-PAMAM Nanostructures. Porphyrin/**G5** nanostructures in the solid state were studied by AFM. The samples were prepared by drop casting at the basal plane of HOPG and imaged in a tapping mode.

G5 alone deposited on the HOPG substrate appears as globular particles (Figure 9). Typical surface coating is about 5%, aggregate heights ranging from 2 to 7 nm, and diameter 20 to 60 nm. The size of **G5** molecules in a neutral water solution measured by light scattering is 5.7 nm in diameter.[41] The Monte Carlo simulations predicted that the size of the dendrimer may change by a factor of up to 1.8, depending on the solution pH and salt concentration.[42] However, a strong **G5**-graphite interaction causes a spherically symmetric dendrimer to adopt an oblate shape on the HOPG surface, as shown in Figure 9. Also note the preferential deposition of aggregates on the steplike inhomogeneities in the HOPG surface.

TPPS alone is known to self-assemble in an acidic aqueous solution (pH ≈ 1) into rods with a well-defined height of several nm and lengths ranging from 0.2 to 2 μm.[9,43] Figure 10a shows a typical AFM image acquired upon deposition of a **G5**-**TPPS** mixture on the HOPG surface at pH 0.7. One can see randomly deposited rod (J-aggregates of **TPPS**) as well as globular **G5** particles. The lateral sizes of the rods are typically larger (20−50 nm) than axial sizes (heights 1.5−5 nm), indicating the formation of ribbonlike structures. These results are in direct agreement with RLS data that also show the formation of large aggregates consisting of a large number of porphyrin units. Interestingly, the AFM image also shows large, irregular clusters that appear to be consisting of several aggregated **G5** molecules. Such aggregation may be caused by porphyrin-induced bridging mediated by the electrostatic attraction between the protonated amine groups of **G5** and negatively charged peripheral substit-

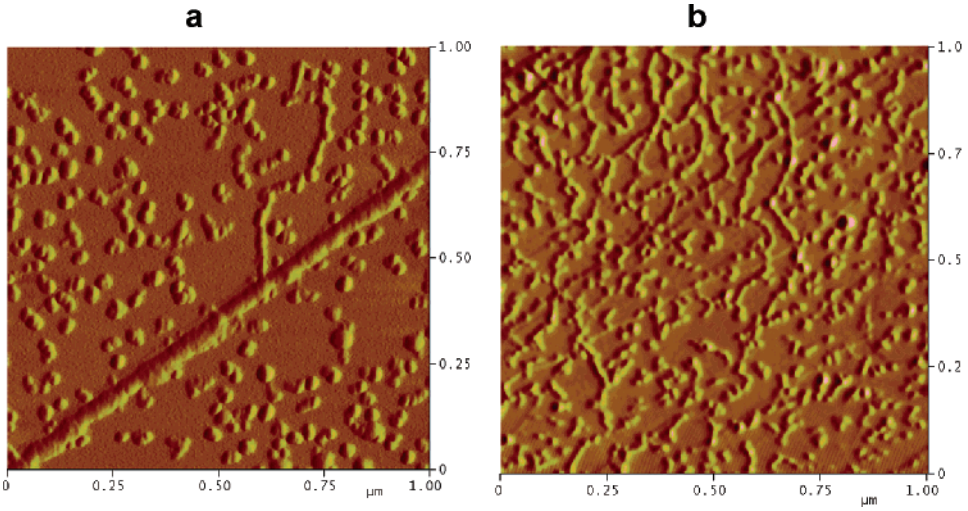

Figure 10. AFM tapping mode image of nanostructures formed by drop casting of acidic aqueous solution (pH 0.7) of 11.1 μM **TPPS** and 3.5 μM **G5** (a), 11.1 μM **TPPP** and 3.5 μM **G5** (b), incubation time 2 h, on basal plane HOPG substrate.

uents of the porphyrin that are not included in the porphyrin rods.

TPPP and **G5** deposited on HOPG at pH 0.7 (Figure 10b) form different nanostructures compared to **TPPS**. Individual **G5** globular formations are connected by bridges consisting of porphyrin self-assembled nanostructures. Both AFM and RLS indicate that the size of the assemblies is smaller while the combination of AFM and the UV−vis spectra (Figure 6) suggests a more random orientation of the porphyrin units in the individual aggregates.

In conclusion, we demonstrated how the delicate balance of acido-basic equilibria and subtle changes in the environment pH define nanoscopic behavior of the porphyrin-dendrimer assemblies. We have shown that pH may be used to achieve association and incorporation of porphyrin assemblies within PAMAM dendrimers and generate porphyrin aggregates and assemblies both in solution and in solid state. Further studies of these features aimed at investigation of assembly/disassembly processes at biological conditions are currently under way. We are hopeful that this study provides insight into a potential application of poly(amidoamine) dendrimers as porphyrin transport agents in medical applications.

Acknowledgment. This research was supported by the Czech Science Foundation (Grant No. 203/04/0426). P.A. gratefully acknowledges support from the Alfred P. Sloan Foundation, Kraft Foods, Inc., and the NSF (NER No. 0304320, SENSOR No. 0330267 to P.A.).

LA051106G

(40) Kubát, P.; Lang, K.; Mosinger, J.; Wagnerová, D. M. *Z. Phys. Chem.* **1999**, *210*, 243−256.
(41) Li, J.; Piehler, L. T.; Qin, D.; Baker, J. R., Jr.; Tomalia, D. A. *Langmuir* **2000**, *16*, 5613−5616.
(42) Welch, P.; Muthukumar, M. *Macromolecules* **1998**, *31*, 5892−5897.
(43) Maiti, N. C.; Mazumdar, S.; Periasamy, N. *J. Porphyrins Phthalocyanines* **1998**, *2*, 369−376.